Electronic Supplementary Information (ESI)

Giant {Mo_{132}}-polyoxometalate isolated with diverse organic cations: a systematic proton conductivity study

Parvathy M. Unnikrishnan, † Olivia Basu, † Rajendar Nasani, Samar K. Das*

School of Chemistry, University of Hyderabad, Hyderabad – 500046, India

*Email: skdas@uohyd.ac.in , samar439@gmail.com

† These authors contributed equally

Table of contents

Sections	Details	Page No.
S1	Experimental procedures	S2
S2	Results and discussion	S3
	S2.1. FT-IR spectrum of methyl viologen	S3
	S2.2. LC-MS data of methyl viologen	S3
	S2.3. Unit cell parameters	S4
	S2.4. PXRD analysis	S4
	S2.5 Morphology of {Mo_{132}}	S5
	S2.6 FT-IR spectra of Mo_{132} products	S6
	S2.7. UV-Visible spectroscopic analysis	S7
	S2.8 XPS analysis	S8-S9
	S2.9 Thermogravimetric analysis	S9
	S2.10. ICP-OES analysis and calculations	S10
	S2.11. CHN analysis and calculations	S10-S14
	S2.12. Proton conductivity studies	S15-S21
	S2.13 Cubic unit cell packing of {Mo132}	S22
	S2.13. Dynamic Vapor sorption studies	S23
	S2.14. Stability check after impedance measurements: Powder X ray diffraction and Fourier transformed infrared spectroscopy	S24-S25
	S2.15. Electrical conductivity study	S25-S27
	S2.16.Comparison of proton conductivity of previously reported POMs	S28
	References	

Section S1. Experimental procedures

Chemicals

All chemicals were used as it is without any additional purification. Ammonium molybdate tetrahydrate ($(NH_4)_6Mo_7O_{24}.4H_2O$), ammonium acetate (CH_3COONH_4), hydrazine sulphate ($N_2H_4.H_2SO_4$) and glacial acetic acid (CH_3COOH) were purchased from SRL chemicals. L- histidine ($C_6H_9N_3O_2$) and 4,4' bipyridyl ($C_{10}H_8N_2$) were procured from TCI chemicals. Iodomethane (CH_3I) was purchased from Sigma Aldrich; pyridine (C_5H_5N), ethyl acetate ($C_4H_8O_2$) and acetonitrile (CH_3CN) from FINAR chemicals.

Synthesis of {Mo_{132}}

{Mo_{132}}: $(NH_4)_{42}$ [$Mo^{VI}_{72}Mo^{V}_{60}O_{372}(CH_3COO)_{30}(H_2O)_{72}$] ca. 300 H_2O ca. 10 CH_3COONH_4

{Mo_{132}} was synthesised following a previous literature[1]. 5.6 g ammonium molybdate (4.5 mmol) was dissolved in 250 ml water. To this, 12.5 g of ammonium acetate (162.2 mmol) was added while stirring, followed by the addition of 0.8 g of hydrazine sulphate (6.1 mmol). At this point, the colour of the solution turned pale green, which then turned to blue, and the blue colour deepened with time. After 10 minutes 83 ml of 50% glacial acetic acid was added to the reaction mixture and stirred for another 20 minutes. This reaction mixture was then kept in rest at 22 °C for four days. Dark brown crystals of {Mo_{132}} were filtered, washed with ethanol and diethyl ether, and dried in air.

Synthesis of Methyl viologen (MV^{2+})

Orange-red colored crystalline methyl viologen (MV^{2+}) was synthesized following a previously reported procedure[2]. Iodomethane (3.5 g, 0.025 mol) was added dropwise to a solution of 4,4'-Bipyridine (1.56 g, 0.01 mol) and acetonitrile (100 ml), while stirring. The reaction contents were refluxed for 24 hours, and ethyl acetate (100 ml) was added after the reaction mixture cooled down to room temperature. The precipitate was filtered, followed by washing with ethyl acetate. Yield: ca. 3.82g, 87%; product analyzed by LC-MS (186.05 $[M]^+$, 93.1 $[M/2]^+$ and FT-IR spectroscopy.

For the synthesis of **His-Mo_{132}**, **Bpy-Mo_{132}**, and **MV-Mo_{132}**, the amount of corresponding organic cations used, that is, histidine (1.5 mmol), bipyridine (1.5 mmol), and methyl viologen (0.75mmol), is less than the amount of pyridine used for the synthesis of corresponding ion-exchanged product **Py-Mo_{132}**, since the solubility of pyridinium ion is higher than the rest of the organic cations used, and all else attained saturation at lower quantity.

Section S2. Results and discussion

Section S2.1. Fourier transformed Infrared spectrum of MV^{2+}

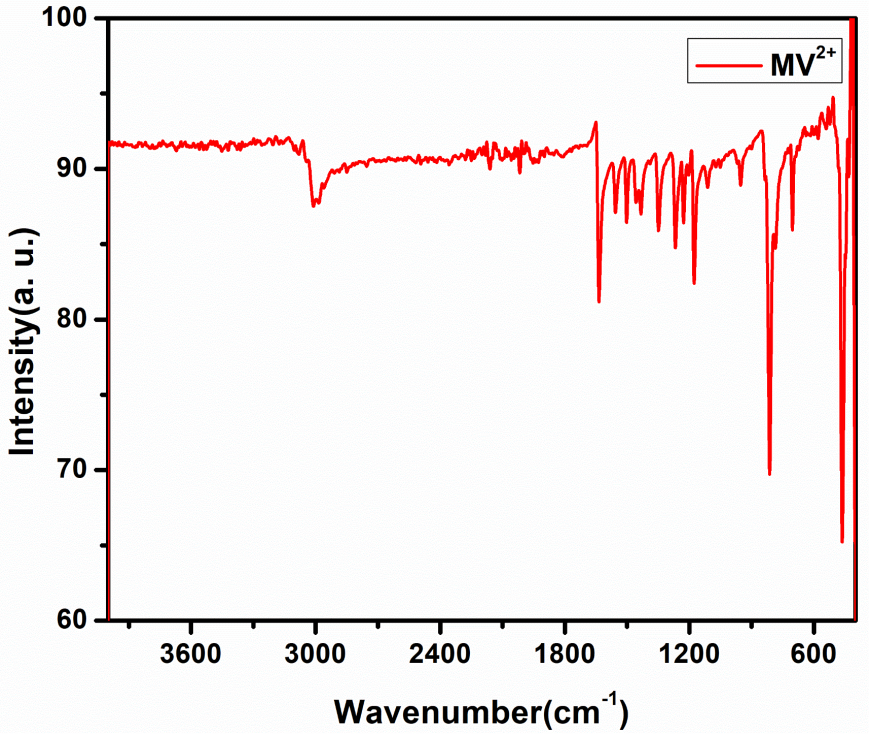

Fig S1. FT-IR spectrum of methyl viologen

Section S2.2. Liquid Chromatography-Mass spectrometric analysis of Methyl viologen

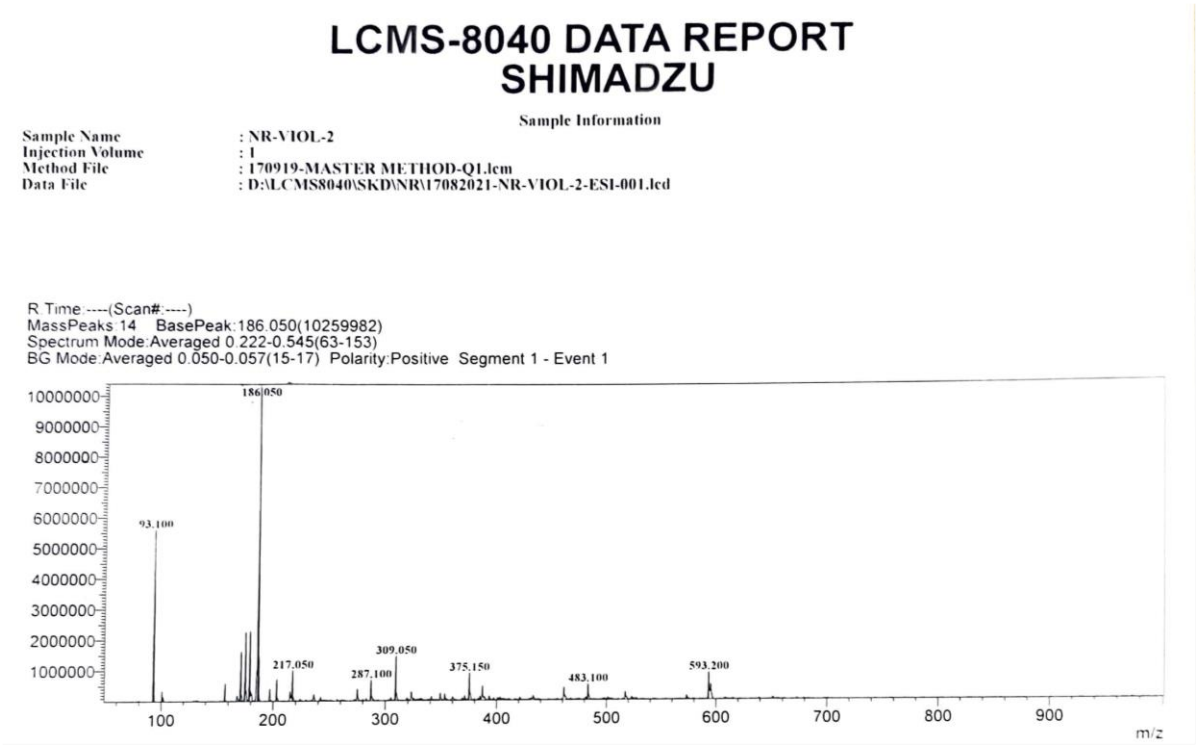

Fig S2. LC-MS data of methyl viologen

Section S2.3. Unit cell parameters of Py-Mo_{132} and His-Mo_{132}

Py-Mo_{132}

Temperature	293K
Wavelength	0.71073 A
Crystal system	Cubic (3)
Unit cell dimensions	a = 44.27 (9) α = 90.1 (2)
	b = 44.42 (10) β = 90.33 (19)
	c = 44.43 (11) γ = 90.03 (18)
Volume	87365 (300)

His-Mo_{132}

Temperature	293K
Wavelength	0.71073 A
Crystal system	Cubic
Unit cell dimensions	a = 44.238 (2) α = 90.0
	b = 44.238 (2) β = 90.0
	c = 44.238 (2) γ = 90.0
Volume	86573 (7)

Section S2.4. Powder X-ray Diffraction analysis

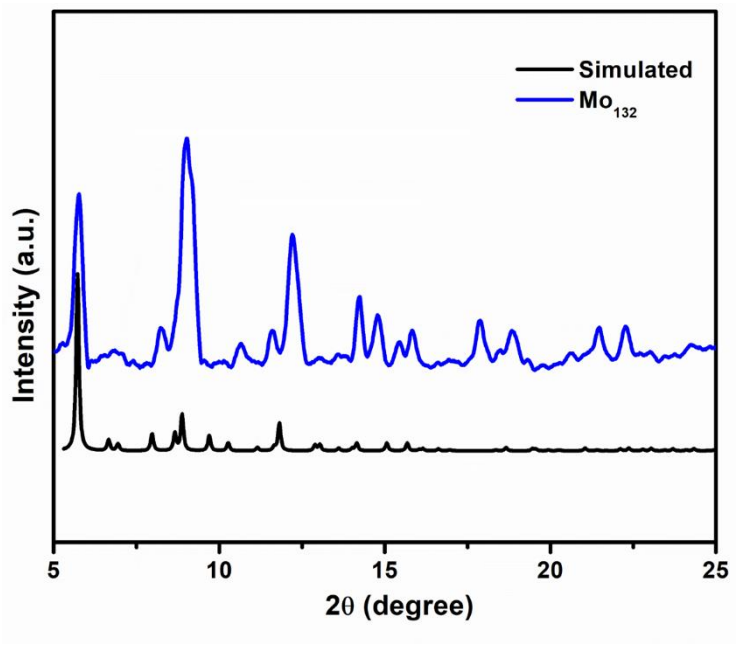

Fig S3. PXRD pattern of synthesized {Mo_{132}} with simulated pattern.

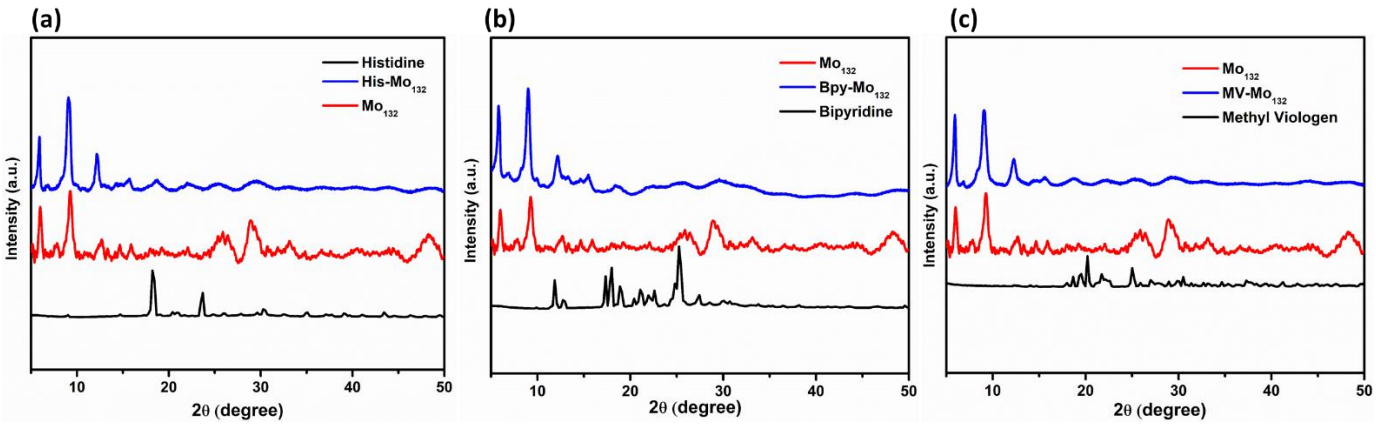

Fig S4. Comparison of the PXRD patterns of (a) His-Mo_{132}, (b) Bpy-Mo_{132}, and (c) MV-Mo_{132}, with the pristine Mo_{132} and respective organic molecules.

Section S2.5. Morphology of {Mo_{132}}

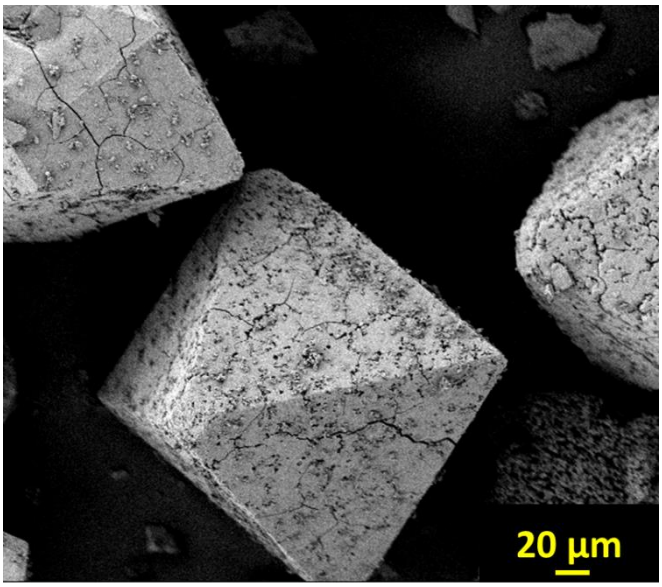

Fig S5. FESEM image of synthesized {Mo_{132}}

Section S2.6. Fourier Transformed Infrared spectroscopic analysis

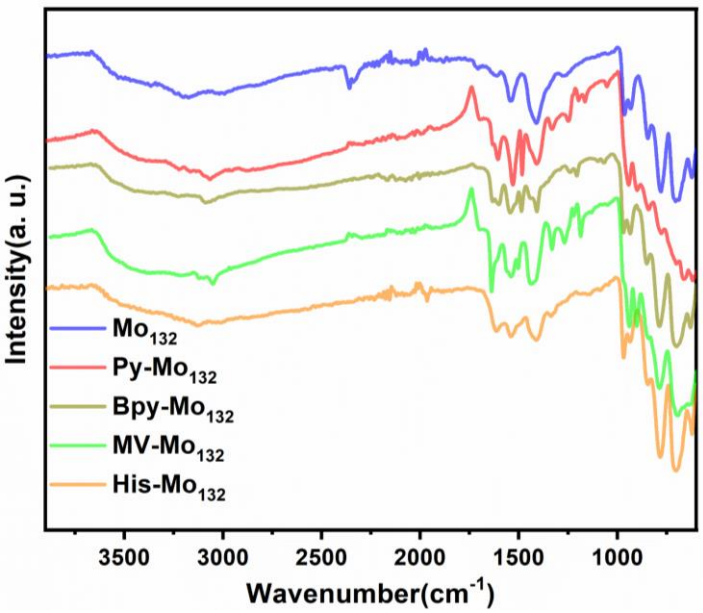

Fig S6. Infrared spectra of {Mo_{132}}, **His-Mo_{132}**, **Py-Mo_{132}**, **Bpy-Mo_{132}**, and **MV-Mo_{132}**

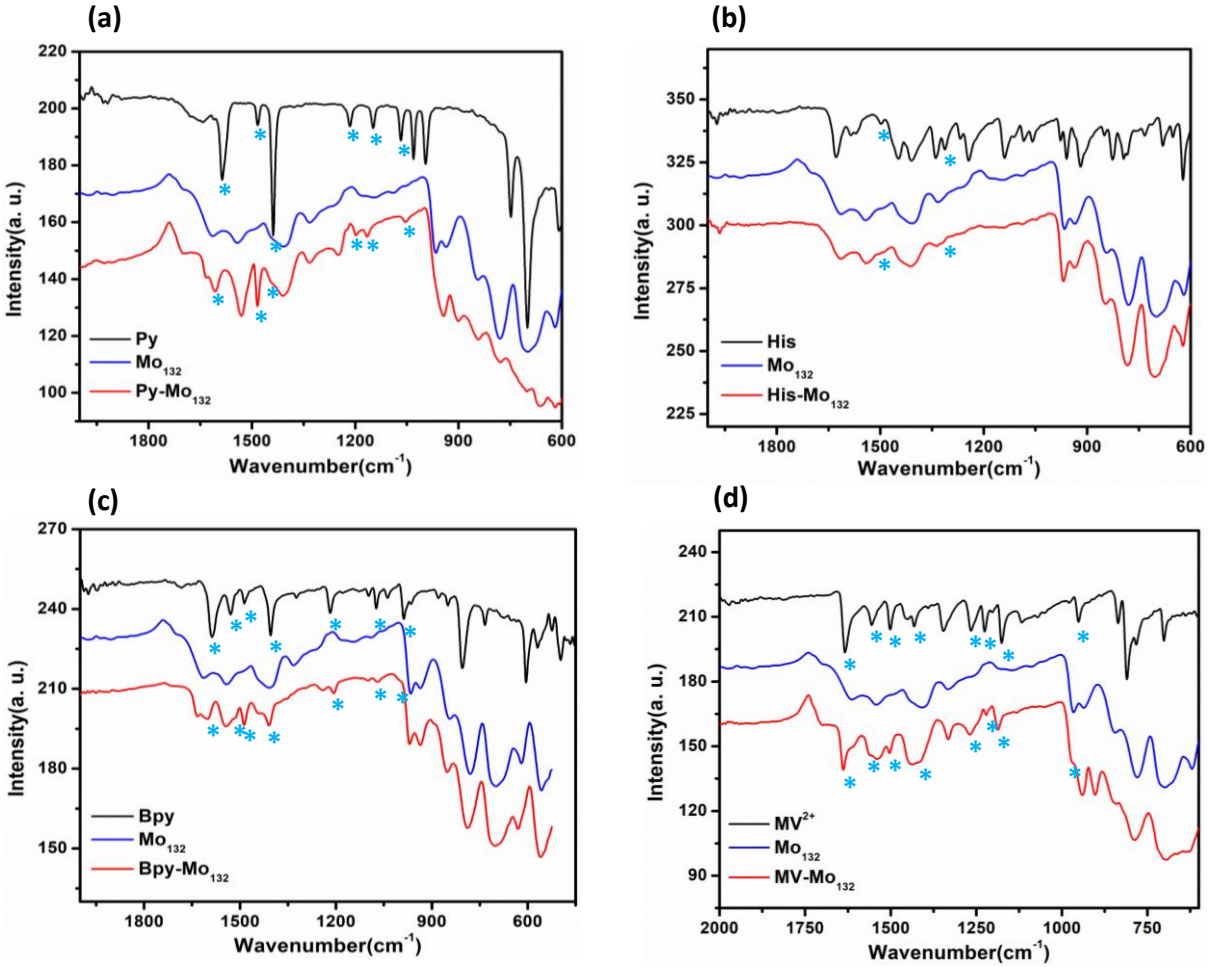

Fig S7. IR spectra of (a) **Py-Mo_{132}**, (b) **His-Mo_{132}**, (c) **Bpy-Mo_{132}**, (d) **MV-Mo_{132}** in comparison with their respective pristine organic molecules and {Mo_{132}}.

Extra peaks in the product caused by organic cations are shown with an asterisk in the figure S5. Each product exhibits peaks corresponding to organic salts, such as the N-H bending mode of aromatic secondary amine at 1480 cm^{-1}, C-N stretching at 1250 cm^{-1}, aromatic C=C ring stretching in the range of 1600cm^{-1}, -C-H aromatic out of plane bending at 980 cm^{-1}. These results demonstrate that these materials are not a composite with pristine {Mo132}

Section S2.7. UV-Visible absorption spectroscopic analysis

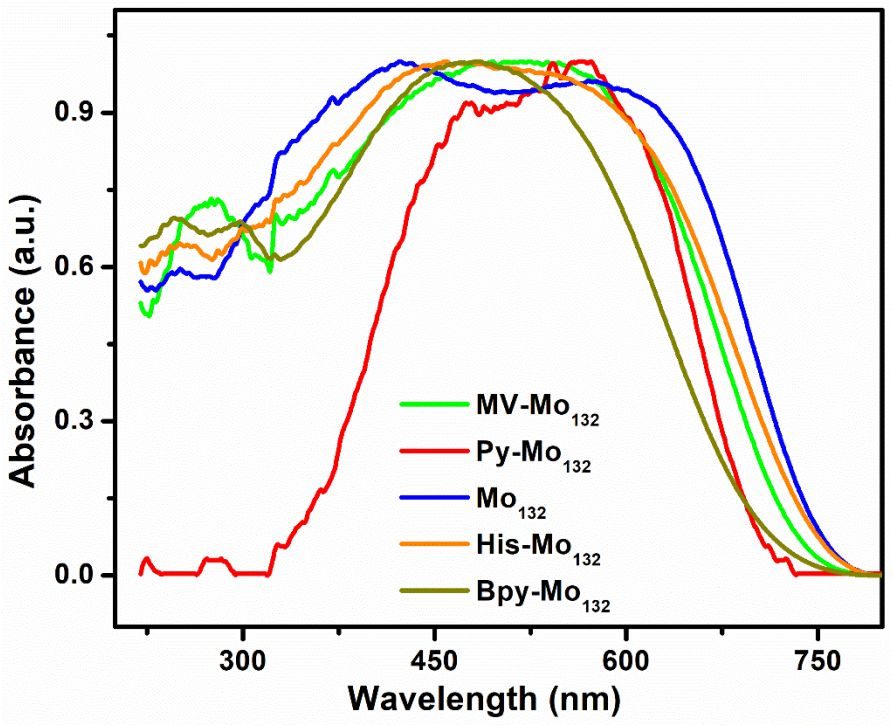

Fig S8. Kubelka-Munk transformed absorption spectra of {Mo_{132}}, **His-Mo_{132}**, **Py-Mo_{132}**, **Bpy-Mo_{132}**, and **MV-Mo_{132}**.

Section S2.8. X-ray photoelectron spectroscopic analysis.

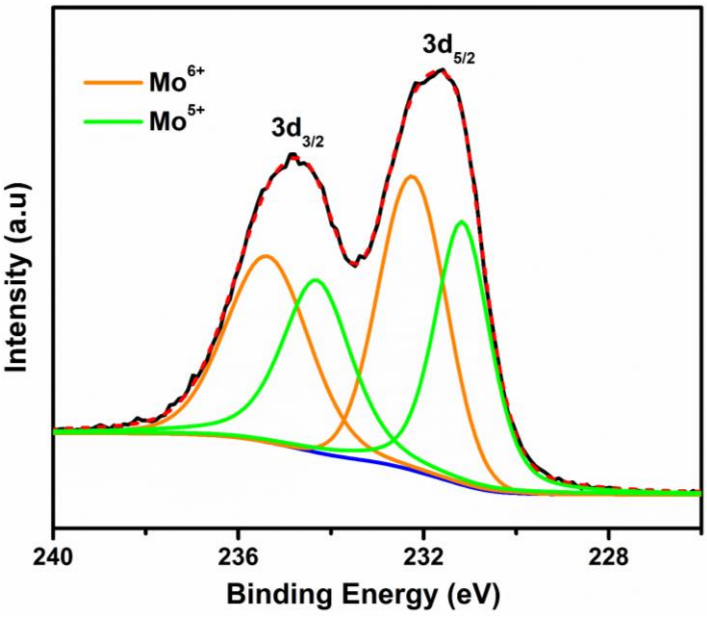

Fig S9. XPS spectrum of **His-Mo$_{132}$.**

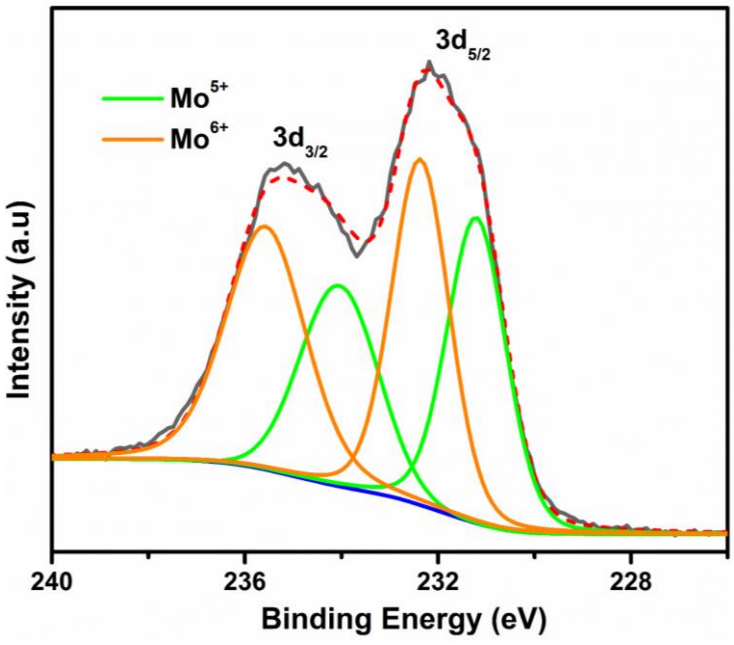

Fig S10. XPS spectrum of **MV-Mo$_{132}$.**

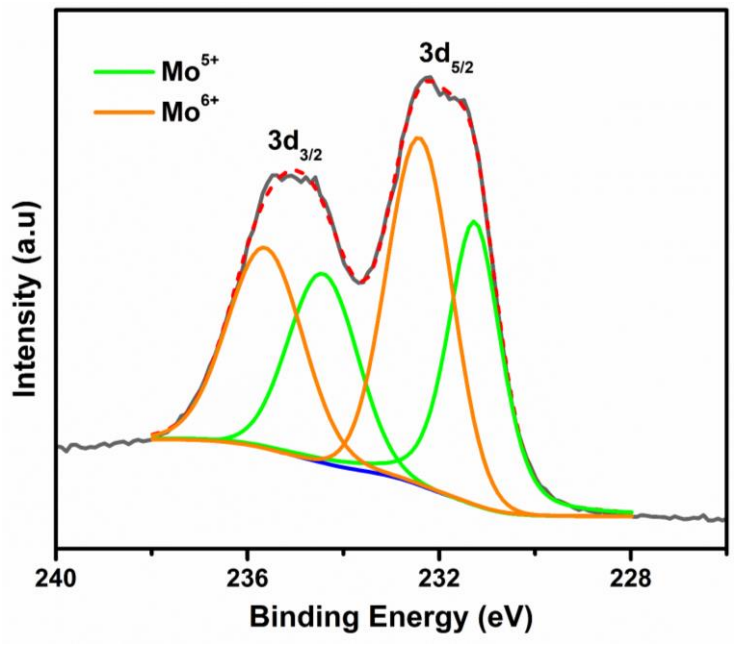

Fig S11. XPS spectrum of **Bpy-Mo$_{132}$.**

Section S2.9. Thermogravimetric analysis

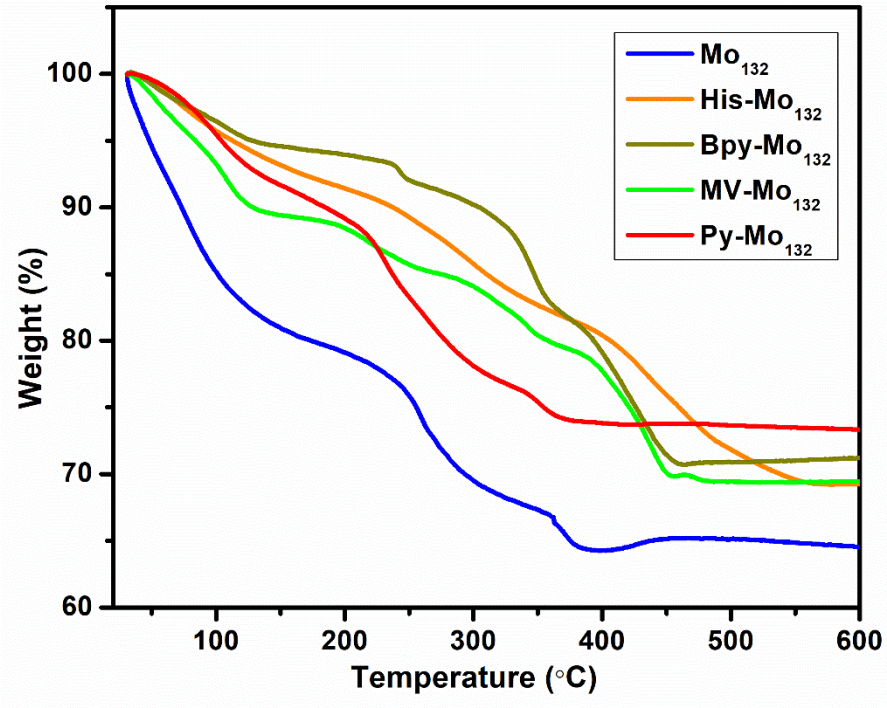

Fig S12. TGA of {Mo$_{132}$}, **His-Mo$_{132}$**, **Py-Mo$_{132}$**, **Bpy-Mo$_{132}$**, and **MV-Mo$_{132}$**.

Section S2.10. ICP-OES elemental analysis

The number of respective organic cations present in **His-Mo$_{132}$**, **Py-Mo$_{132}$**, **Bpy-Mo$_{132}$**, and **MV-Mo$_{132}$**, were calculated from CHN and ICP-OES elemental analysis; the calculations of which are provided below.

Table S1. Result of ICP-OES analysis for Mo.

Compounds	Sample provided (mg)	Concentration (ppm)
Bpy-Mo$_{132}$	13.1	155.2
Py-Mo$_{132}$	13.6	180
His-Mo$_{132}$	13.8	164.2
MV-Mo$_{132}$	13.4	175.7

Calculation of amount of Mo in each sample

Molar mass of Molybdenum = 95.95

For **Bpy-Mo$_{132}$**, number of moles of Mo in the analyzed sample solution = 1.617×10^{-3} in 1 L

The sample was provided in 4 ml HCl, which then diluted 10 times before analysis.

Thus, in 40 ml of the sample, number of moles of Mo = 6.470×10^{-5}

Mass of Mo in 100 g of **Bpy-Mo$_{132}$** sample = 47 g

Similarly calculated for other samples as well and obtained as 52 g Mo in **Py-Mo$_{132}$**, 52.4 g Mo in **MV-Mo$_{132}$** and 47.5 g of Mo in **His-Mo$_{132}$**.

SOPHISTICATED ANALYTICAL INSTRUMENT FACILITY
IIT MADRAS, CHENNAI-36
PERKIN ELMER OPTIMA 5300 DV ICP-OES

Sample code	Element symbol and Wavelength (nm)	Dilution Factor	Concn.in ppm µg/ml (or) mg/litre
1	Mo 202.031	10	155.2 mg/L
2	Mo 202.031	10	163.1 mg/L
3	Mo 202.031	10	180.0 mg/L
4	Mo 202.031	10	164.2 mg/L
5	Mo 202.031	10	175.7 mg/L

Fig S13. Inductively coupled plasma (ICP-OES) analysis of **His-Mo$_{132}$**, **Py-Mo$_{132}$**, **Bpy-Mo$_{132}$**, and **MV-Mo$_{132}$** and {Mo$_{132}$}

Section S2.11. CHN elemental analysis

Table S2. Result of CHN analysis.

Compounds	C (%)
His-Mo$_{132}$	10.08
Py-Mo$_{132}$	9.80
Bpy-Mo$_{132}$	13.79
MV-Mo$_{132}$	11.01
{Mo$_{132}$}	4.33

The molecular formula of all products according to the CHN and ICP analysis are as follows

- **Py-Mo$_{132}$:** $(NH_4)_{13}(PyH)_{29}[Mo^{VI}_{72}Mo^{V}_{60}O_{372}(CH_3COO)_{30}(H_2O)_{72}]\cdot 67H_2O\cdot 10CH_3COONH_4$
- **His-Mo$_{132}$:** $(NH_4)_{20}(HisH)_{22}[Mo^{VI}_{72}Mo^{V}_{60}O_{372}(CH_3COO)_{30}(H_2O)_{72}\cdot 110H_2O\cdot 10CH_3COONH_4$
- **Bpy-Mo$_{132}$:**
  $(NH_4)_{18}(BpyH)_{24}[Mo^{VI}_{72}Mo^{V}_{60}O_{372}(CH_3COO)_{30}(H_2O)_{72}]\cdot 128H_2O\cdot 10CH_3COONH_4$
- **MV-Mo$_{132}$:** $(NH_4)_{14}(MV)_{14}[Mo^{VI}_{72}Mo^{V}_{60}O_{372}(CH_3COO)_{30}(H_2O)_{72}]\cdot 84H_2O\cdot 10CH_3COONH_4$

Document: 14.08.2024 (varioMICRO) from: 14-08-24 10:00 PM

analytic functional testing
varioMICRO CHNS PV
serial number: 15181026

Graphic report

No.	Name	N [%]	C [%]	H [%]	S [%]	Date Time
19	UP-M0132	2.84	4.33	3.120	0.158	14-08-24 03:15 PM

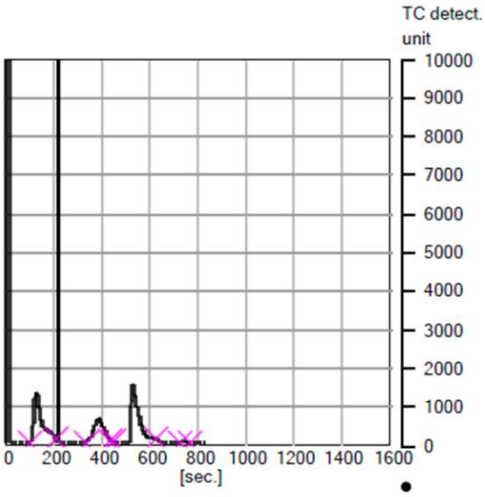

Fig S14. CHN data of {Mo_{132}}.

No.	Name	N [%]	C [%]	H [%]	S [%]	Date Time
22	UP-PY	1.63	9.80	2.696	0.091	14-08-24 03:58 PM

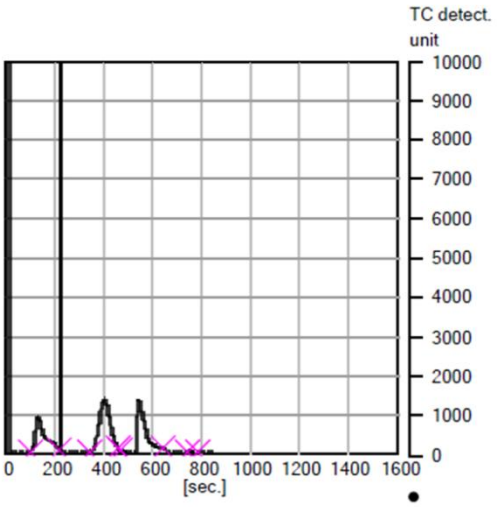

Fig S15. CHN data of **Py-Mo_{132}**.

No.	Name	N [%]	C [%]	H [%]	S [%]	Date Time
23	UP-HIS	4.42	10.08	2.698	0.055	14-08-24 04:12 PM

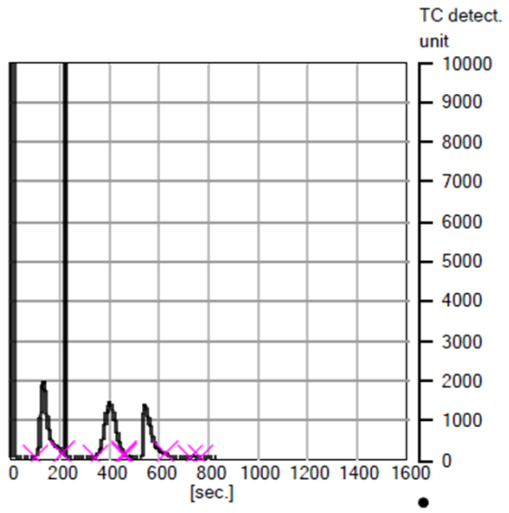

Fig S16. CHN data of **His-Mo$_{132}$**.

No.	Name	N [%]	C [%]	H [%]	S [%]	Date Time
20	UP-MV	1.70	11.01	2.865	0.119	14-08-24 03:29 PM

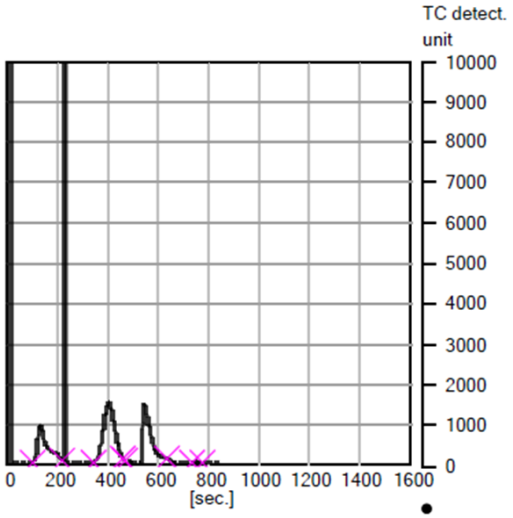

Fig S17. CHN data of **MV-Mo$_{132}$**.

No.	Name	N [%]	C [%]	H [%]	S [%]	Date Time
21	UP-BPY	3.02	13.79	2.634	0.080	14-08-24 03:44 PM

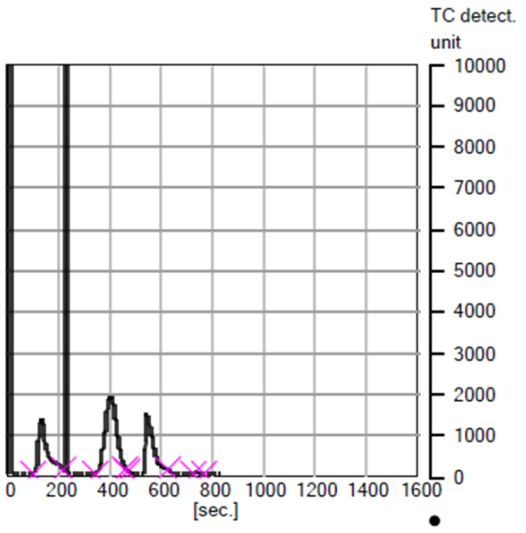

Fig S18. CHN data of **Bpy-Mo$_{132}$.**

Section S2.12. Proton conductivity studies

Py-Mo_{132}

Table S3. Proton conductivity values of Py-Mo_{132} at different temperatures.

Temperature (°C)	Conductivity (Scm^{-1})
35	0.003
40	0.004
50	0.0051
60	0.0068
70	0.0083
80	0.0107

Table S4. Proton conductivity values of Py-Mo_{132} at 45 °C and different relative humidity.

Relative humidity (%)	Conductivity (Scm^{-1})
98	0.0063
90	0.0059
85	0.0051
80	0.0049
75	0.0047
70	0.0044

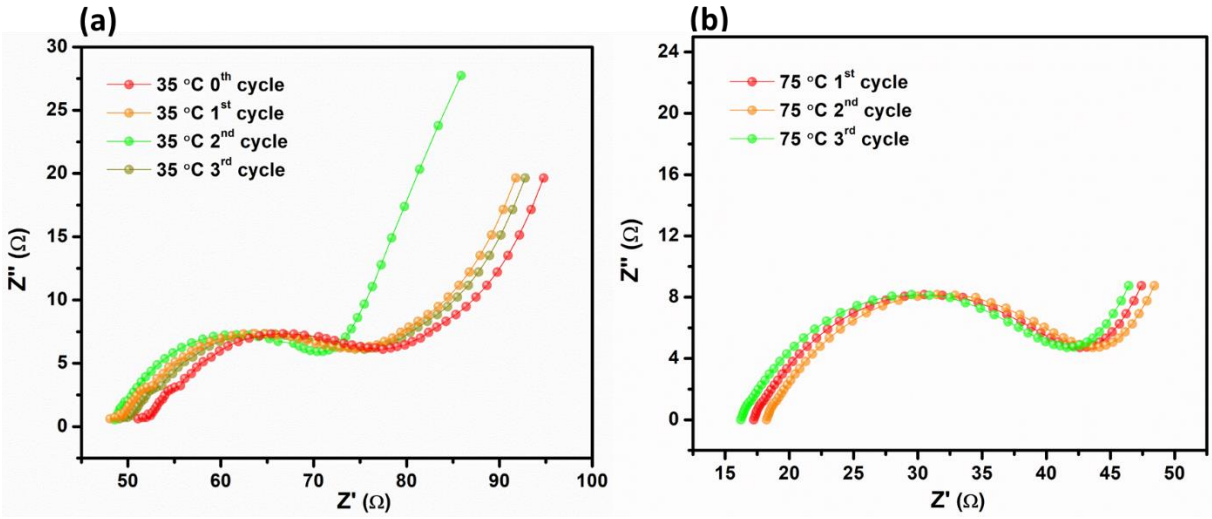

Fig S19. Nyquist plots for **Py-Mo_{132}** at constant relative humidity of 98% and (a) at 35 °C and (b) at 75 °C.

His-Mo$_{132}$

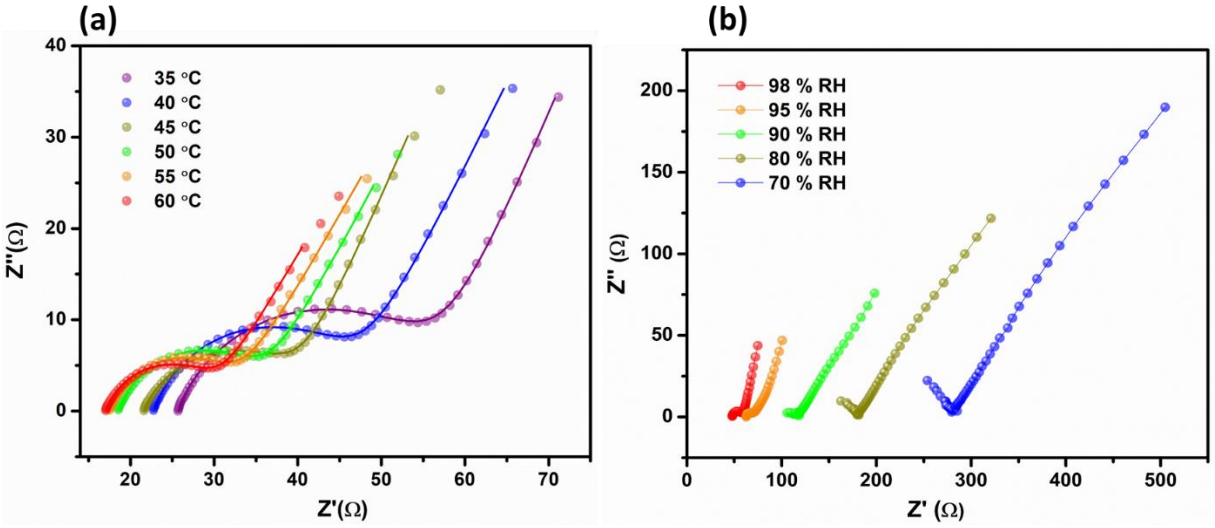

Fig S20. Nyquist plots for **His-Mo$_{132}$** at (a) 98% RH and different temperatures; (b) at 45 °C and different RH. The solid line represents the fitted data, and the points denote the experimental data.

Table S5. Proton conductivity values of His-Mo$_{132}$ at different temperatures.

Temperature (°C)	Conductivity (Scm^{-1})
35	0.0044
40	0.0050
45	0.00528
50	0.00611
55	0.00653
60	0.00669

Table S6. Proton conductivity values of His-Mo$_{132}$ at 45 °C and different relative humidity.

Relative Humidity (%)	Conductivity (Scm^{-1})
98	0.0032
95	0.0024
90	0.0015
80	0.0009
70	0.0006

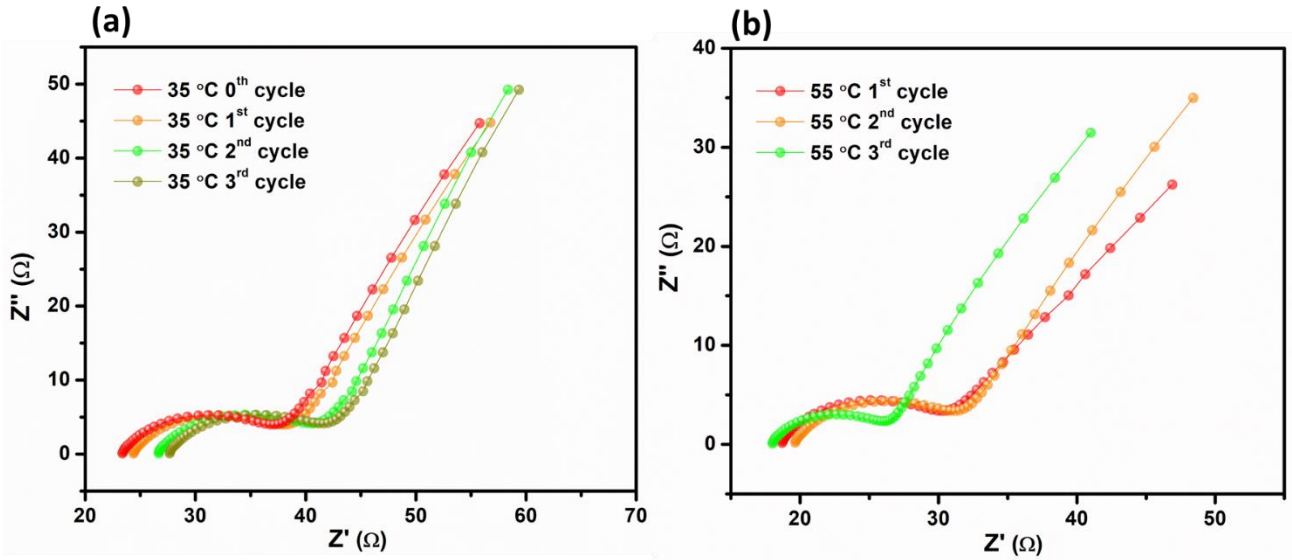

Fig S21. Nyquist plots for **His-Mo$_{132}$** at constant relative humidity of 98% and (a) at 35 °C (b) and at 55 °C.

Bpy-Mo$_{132}$

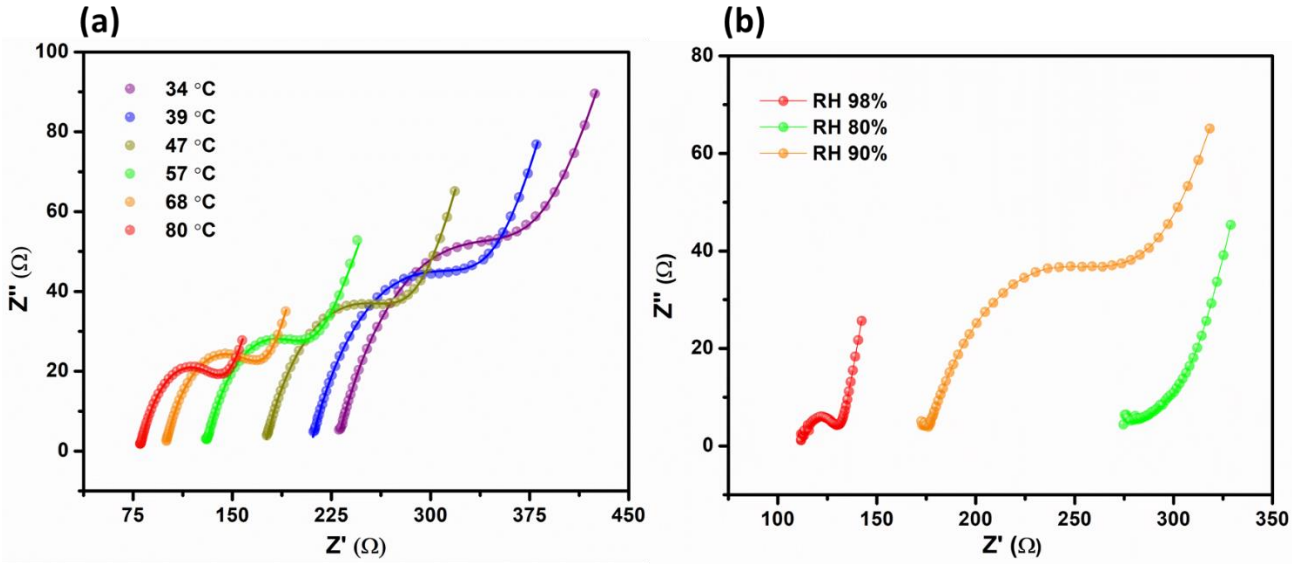

Fig S22. Nyquist plots for **Bpy-Mo$_{132}$** (a) at 98% RH and different temperatures; (b) at 45°C and different RH. The solid line represents the fitted data, and the points denote the experimental data.

Table S7. Proton conductivity values of Bpy-Mo_{132} at different temperatures.

Temperature (°C)	Conductivity (Scm^{-1})
34	0.00070
39	0.000769
47	0.00095
57	0.00122
68	0.00168
78	0.002

Table S8. Proton conductivity values of Bpy-Mo_{132} at 50 °C and different relative humidity.

Relative Humidity (%)	Conductivity (Scm^{-1})
98	0.0013
90	0.00085
80	0.0006

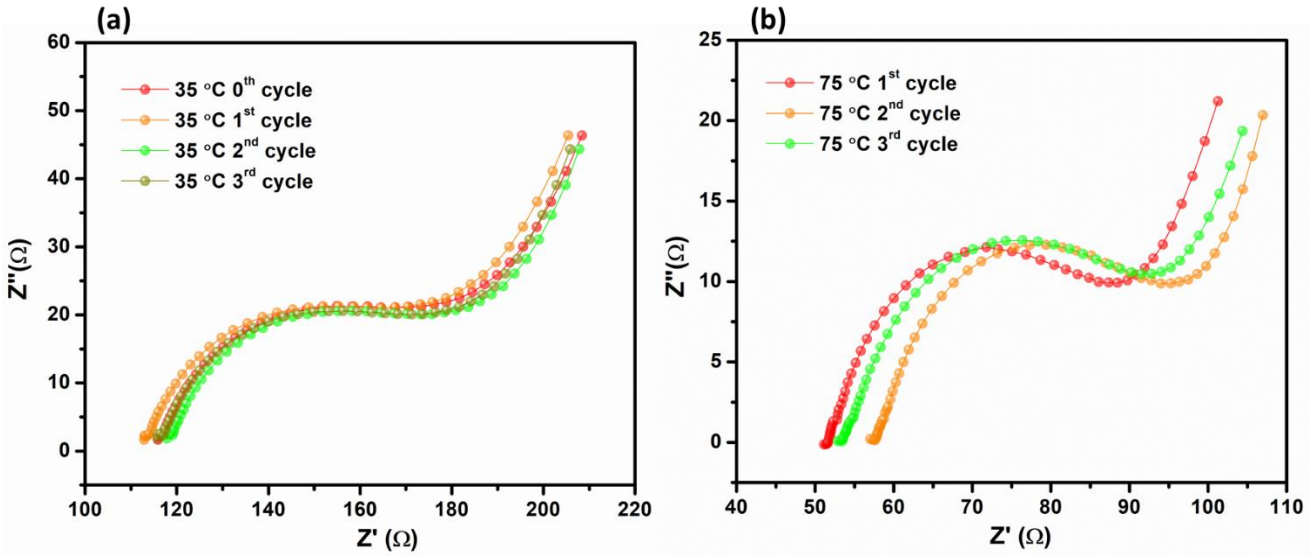

Fig S23. Nyquist plots for **Bpy-Mo_{132}** at constant relative humidity of 98% and (a) at 35 °C (b) and at 75 °C.

MV-Mo$_{132}$

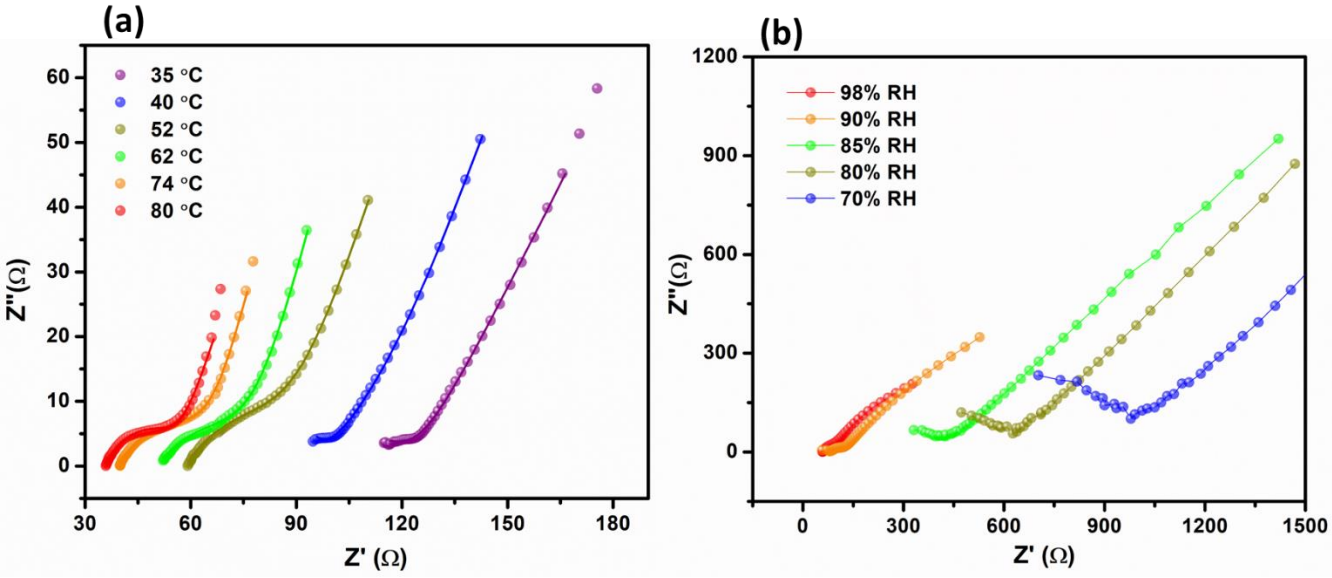

Fig S24. Nyquist plots for **MV-Mo$_{132}$** at (a) 98% RH and different temperatures; (b) at 45 °C and different RH. The solid line represents the fitted data, and the points denote the experimental data.

Table S9. The proton conductivity values of MV-Mo$_{132}$ at different temperatures.

Temperature (°C)	Conductivity (Scm^{-1})
35	0.0012
40	0.00142
52	0.00219
62	0.00272
74	0.00349
81	0.00389

Table S10. Proton conductivity values of MV-Mo$_{132}$ at 50 °C and different relative humidity.

Relative Humidity (%)	Conductivity (Scm^{-1})
98	0.0026
90	0.0016
85	0.00046
80.	0.00032
75	0.00025

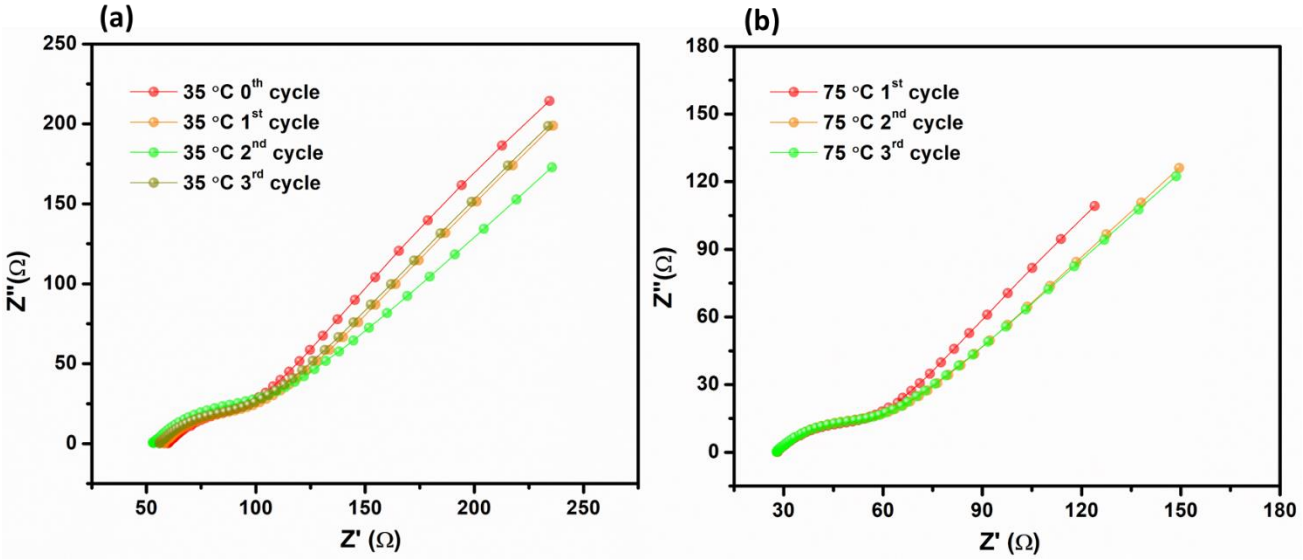

Fig S25. Nyquist plots for **MV-Mo$_{132}$** at constant relative humidity of 98% and (a) at 35 °C (b) and at 75 °C.

Calculation of proton conductivity: Using EC-Lab software, the proton conductivity of all the four products was calculated from the respective Nyquist plots after being fitted to the most appropriate equivalent circuit.

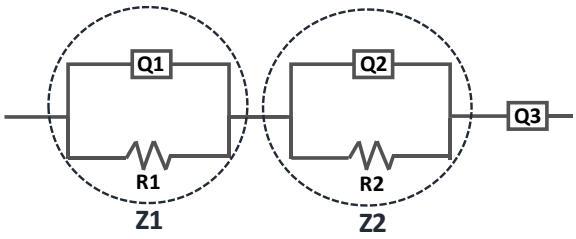

Fig S26. Equivalent electrical circuit used for fitting the experimentally obtained Nyquist plots.

Figure S23 shows the equivalent circuit used for fitting the data of these four products. The circuit consists of three major parts, Z1, Z2, and Q3. Z1 corresponds to the pellet impedance and is composed of two elements R1 and Q1. Here R1 accounts for the bulk resistance of the sample pellet, which can be got from the smaller semicircle in the high frequency region of the Nyquist plot. Similarly, R2 accounts for the charge transfer resistance existing between the sample pellet electrolyte and the electrode which is determined from the larger semicircle. Q1, Q2 and Q3 are the constant phase elements, where Q1 and Q2 represents the non-ideal capacitance in bulk and Q3 accounts for the non-ideal capacitance of electrode-electrolyte interface.

Thus, the value of R1, which is in this case refers to the resistance observed during proton conduction, was obtained by fitting the experimentally obtained data points to the equivalent circuit chosen.[3,4]

Calculation of proton conductivity from R1:

Proton conductivity **(σ) = l/AR**

l = Thickness of the pellet

A = Area of cross section of the pellet

R = Resistance

For example,

R1 for **Py-Mo$_{132}$**, at 80 °C and 98% humidity = 14 Ω

Thickness of that corresponding pellet = 0.198 cm

Area of cross section of the pellet = 1.32 cm^2

Therefore, proton conductivity (σ) = 0.198/ (1.32 × 14) = 1.07×10^{-2} Scm^{-1}

Calculation of activation energy for proton conduction

Activation energy for proton conductivity is calculated from the proton conductivity values at different temperatures. From the slope of the curve of the plot of 1000/T versus ln(σ T), activation energy can be calculated.

For example,

Consider the plot between 1000/T and ln (σ T) at various temperatures for **Py-Mo$_{132}$**.

The slope of the curve is = −2.8 Scm^{-1}

From the Arrhenius equation**, $\sigma T = \sigma_0 \times e^{-Ea/RT}$**

Where, σ = conductivity of the sample

T = temperature in the kelvin scale

E_a = Activation energy

R = Ideal gas constant = 8.63×10^{-5} eV K^{-1}

This equation can be written as

$\ln(\sigma T) = \ln(\sigma_0) - E_a/RT$, or

$\ln(\sigma T) = \ln(\sigma_0) + (-E_a/1000R \times 1000/T)$

This represents a straight-line plot, and the slope = **$-E_a/1000R$**

Therefore, if slope from plot = $-2.8 Scm^{-1}$

Activation energy $E_a = 2.8 \times 1000 \times 8.63 \times 10^{-5} = 0.24$ eV

Section S2.13. Unit cell packing of {Mo_{132}}

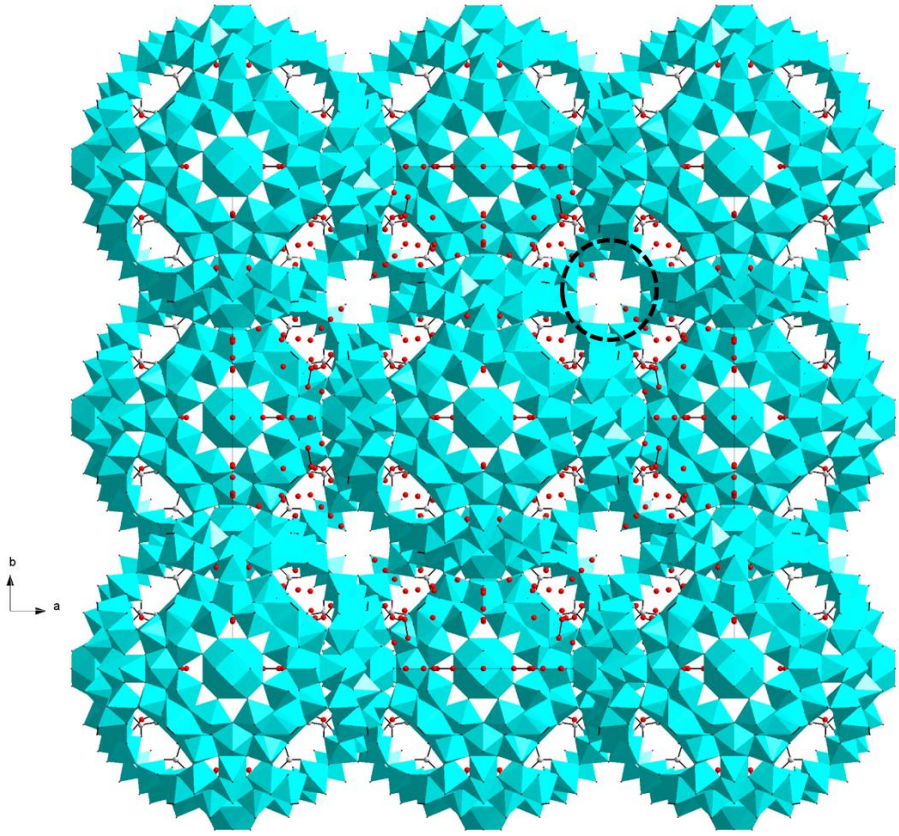

Fig. S27. Unit cell packing of {Mo_{132}} (the black circle shows the void space of 5 Å, which could fit a pyridine molecule but no other organic cations chosen. The crystal packing image was made from the CIF file of parent {Mo_{132}} - *Angew. Chem. Int. Ed.* 1998, **37**, 3359-3363). We have shown, by PXRD studies and by measuring unit cell parameters of two synthesized ion-exchanged compounds, that all these title compounds crystallize in cubic crystal system.

Section S2.14. Dynamic vapor sorption analysis

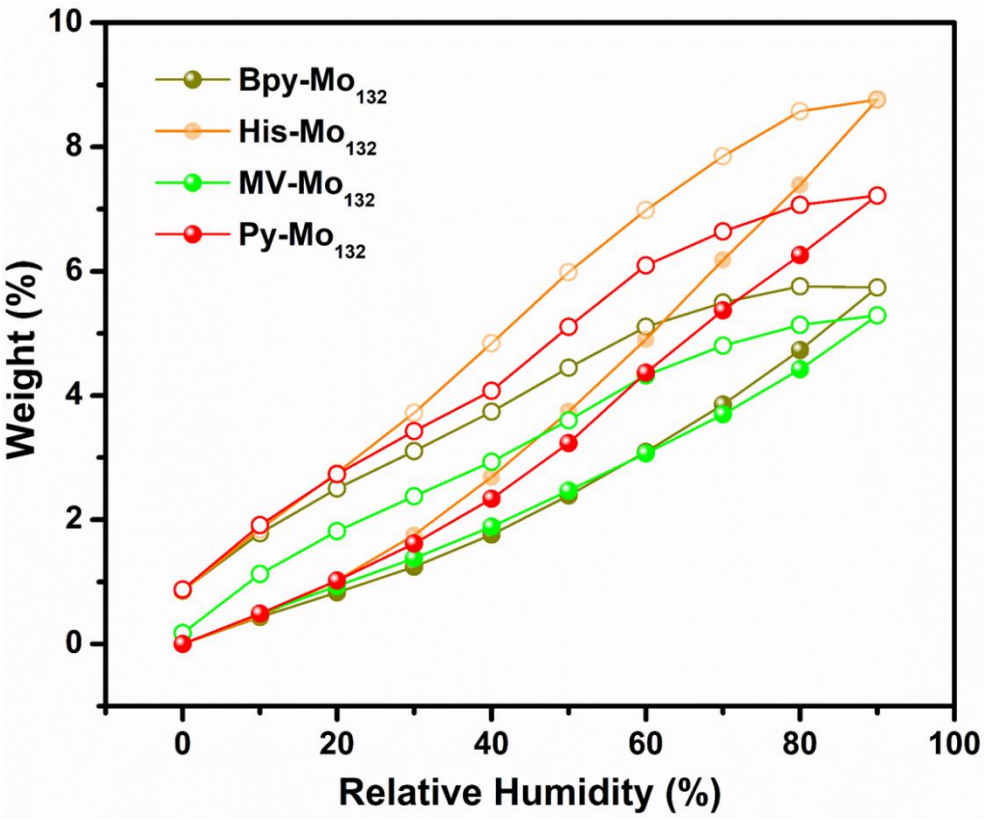

Fig S28. Dynamic vapor sorption isotherms for **His-Mo$_{132}$, Py-Mo$_{132}$, Bpy-Mo$_{132}$, and MV-Mo$_{132}$**

Section S2.15. Stability check after impedance measurements: Powder X ray diffraction (PXRD) and infrared spectroscopy (IR)

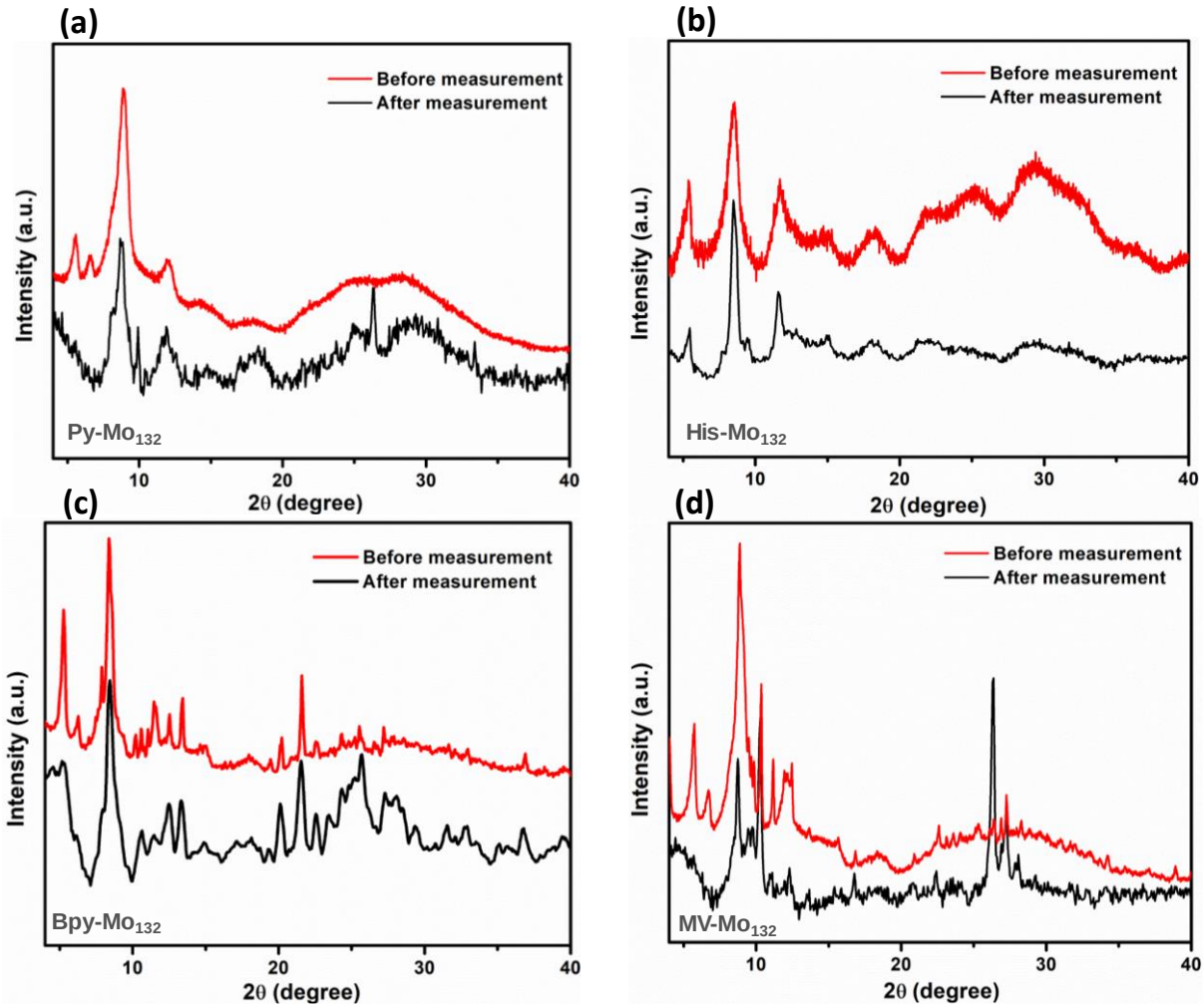

Fig S29. PXRD patterns of (a) **Py-Mo$_{132}$** (b) **His-Mo$_{132}$** (c) **Bpy-Mo$_{132}$** and (d) **MV-Mo$_{132}$**, before and after proton conductivity experiments on the sample pellet. The new peak present at 2θ value of 26 in all the PXRD patterns taken after proton conductivity experiment, is originating from traces of carbon paper present in the sample, prepared by powdering the pellet.

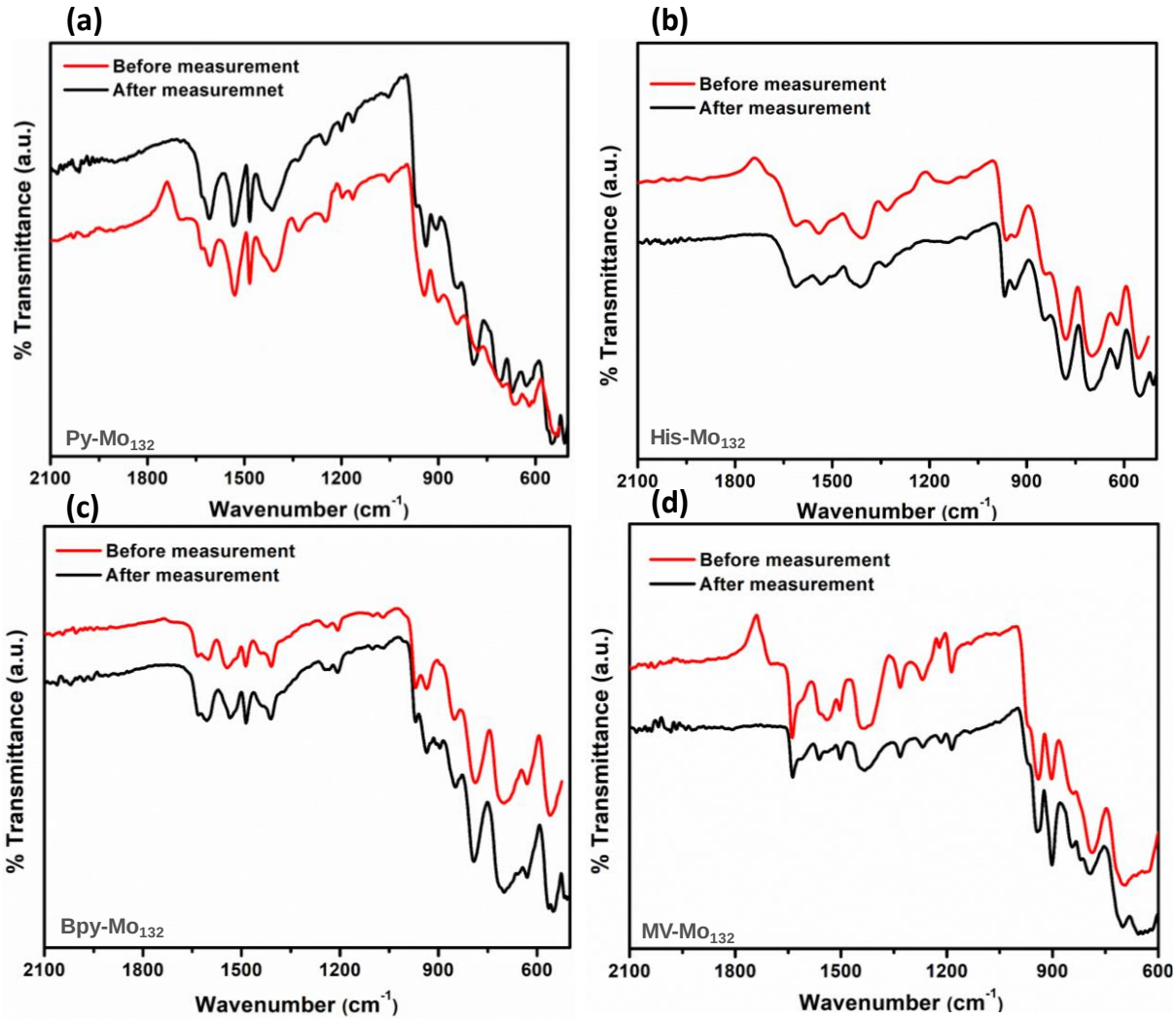

Fig S30. IR spectra of (a) **Py-Mo$_{132}$** (b) **His-Mo$_{132}$** (c) **Bpy-Mo$_{132}$** (d) **MV-Mo$_{132}$**.

Section S2.16 Electrical conductivity study

Experimental setup: The electrical conductivity measurement for all compounds was done using a two-electrode set up, where 10 mg of each sample was placed in a cylindrical cell at room temperature and 25% humidity. All the samples were ground to a fine powder before placing in the cell. Electric current (DC) was allowed to flow through the sample between the two electrodes, and the resistance was measured using Zahner Zanium electrochemical workstation, operated by Thales software.

The corresponding plots of electrical conductivity measurements are provided.

Calculation of electrical conductivity:

The electrical conductivity was calculated from the following equations.

$$\sigma = L/AR$$

$$R=V/I$$

σ = Electrical conductivity
L = Height of the cylindrical cell containing the sample
A = Surface area of the base of the cylindrical cell
R = Resistance
V = Potential
I = Current

For **Py-Mo$_{132}$**,

L=0.07 cm
A= 0.0408 cm^2
V=1 V
I = 2.604×10^{-7} A

Therefore, R= $1/2.604\times10^{-7} = 0.384\times10^{7}$ Ω.
Now, $\sigma = 0.07/ 0.04018 \times 0.384\times10^{7} = 4.5\times10^{-7}$ Scm^{-1}

Table S11. Electrical conductivities of the four products

Sample	Current (A) @ 1V	Resistance (Ω)	Conductivity (Scm^{-1})
Py-Mo$_{132}$	2.604×10^{-7}	0.384×10^{7}	4.5×10^{-7}
His-Mo$_{132}$	2.583×10^{-8}	0.394×10^{8}	5.05×10^{-8}
MV-Mo$_{132}$	2.213×10^{-7}	0.451×10^{7}	4.9×10^{-7}
Bpy-Mo$_{132}$	6.126×10^{-8}	0.16×10^{8}	1.7×10^{-7}

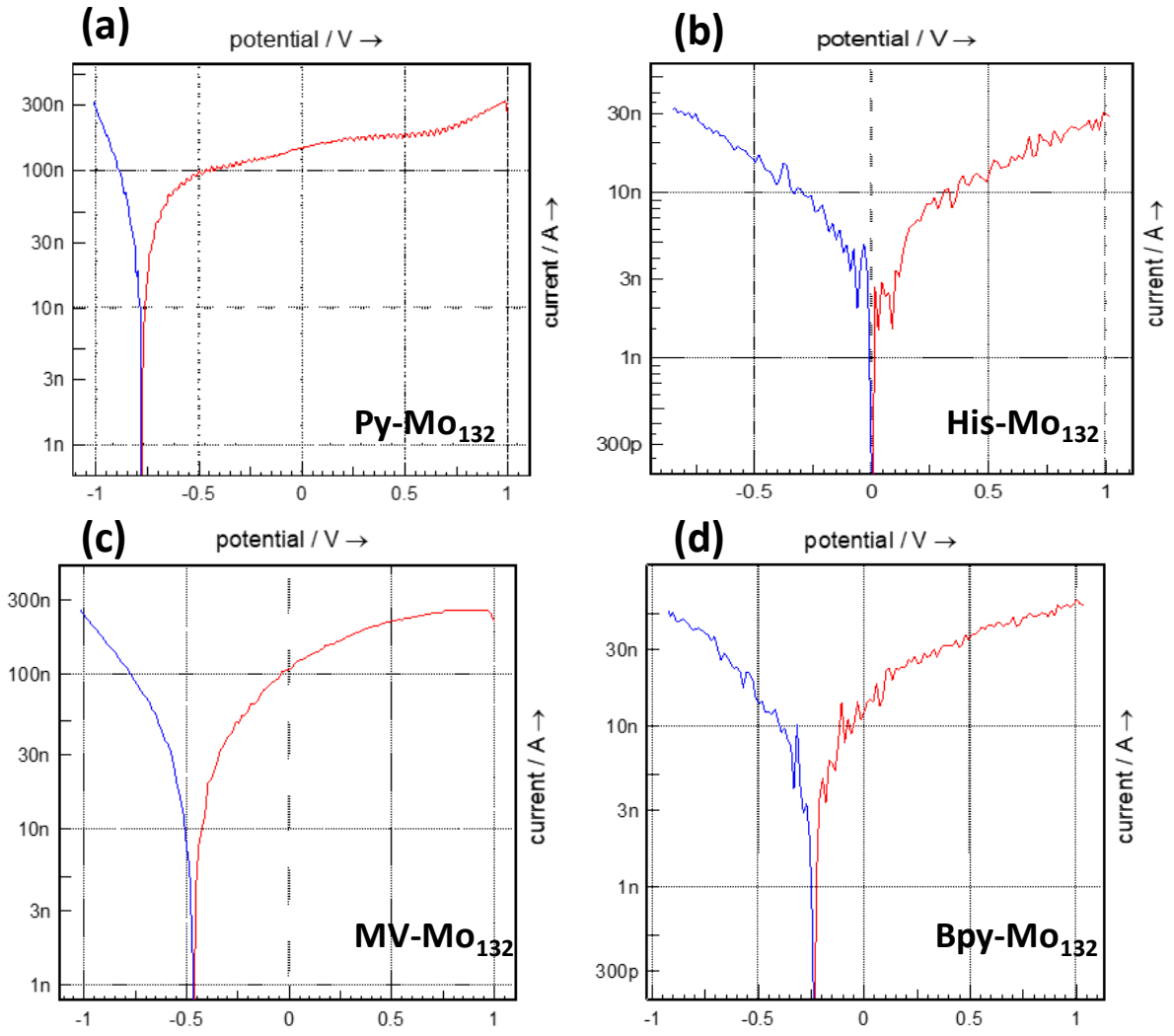

Fig S31. Electrical conductivity measurement (potential vs current) of (a) **Py-Mo$_{132}$**, (b) **His-Mo$_{132}$**, (c) **MV-Mo$_{132}$**, and (d) **Bpy-Mo$_{132}$**.

Section S2.17 Proton conductivity of giant POM-based proton conductors

Table S12. **Proton conductivity of giant POM based proton conductors**

SI No:	Compound	Conductivity	Conditions	Reference
1	$TBAMo_{132}$	1.8×10^{-5}	60°C and 98% RH	6
2	**Bpy-Mo$_{132}$**	1.17×10^{-3}	80°C and 98% RH	**This work**
3	$Mo_{72}Fe_{30}O_{252}(CH_3COO)_{12}\{Mo_2O_7(H_2O)\}_2\{H_2Mo_2O_8(H_2O)\}(H_2O)_{91}]\cdot 150H_2O$	1.85×10^{-3}	57°C and 50% RH	7
4	$ILMo_{132}$	3.28×10^{-3}	60°C and 98% RH	6
5	**MV-Mo$_{132}$**	4.17×10^{-3}	80°C and 98% RH	**This work**
6	**His-Mo$_{132}$**	5.2×10^{-3}	60°C and 98% RH	**This work**
7	$\{(NH_4)_{13}[Mo_{28}{}^{V}Mo_{126}{}^{VI}O_{456}H_{34}(H_2O)_{70}]Cl_{17}(ClO_4)_{14}\cdot mH2O$	1.1×10^{-2}	22°C and 100% RH	8
8	**Py-Mo$_{132}$**	1.1×10^{-2}	80 °C and 98% RH	**This work**
9	$HMeImMo_{132}$	2.13×10^{-2}	60°C and 98% RH	6
10.	$HImMo_{132}$	4.98×10^{-2}	60°C and 98% RH	6
11.	$(NH_4)_{21}H^{+}{}_{59-2x}[Mo^{V}{}_{180}Mo^{VI}{}_{60}\text{-}(OH)60O_{620-x}(SO_3)_{20-x}(SO_4)_x]\cdot ca337H_2O$	1.03×10^{-1}	80°C and 98% RH	9

REFERENCES

(1) A. Müller, E. Krickemeyer, H. Bögge, M. Schmidtmann and F. Peters, *Angew. Chem. Int. Ed*. 1998, **37**, 3359-3363.
(2) M.R. Geraskina, A.S. Dutton, M. J. Juetten, S.A. Wood and A.H. Winter, *Angew. Chem., Int. Ed.* 2017, **56**, 9435-9439.
(3) S. Mukhopadhyay, J. Debgupta, C. Singh, R. Sarkar, O. Basu, S.K. Das, *Appl. Mater. Interfaces* 2019, **11**, 13423−13432.
(4) O. Basu, S. Mukhopadhyay, S. Laha and S.K. Das, *Chem. Mater*. 2022, **34,** 6734−6743.
(5) Y. Zhou, Z. Shi, L. Zhang, S. Hassan and N. Qu, *Appl. Phys. A* 2013, **113**, 563–568.
(6) W. J. Liu, L. Z. Dong, R. H. Li, Y. J. Chen, S. N. Sun, S. L. Li and Y. Q. *ACS Appl. Mater. Interfaces* 2019, **11**, 7030–7036.
(7) K. Tandekar, C. Singh, and S. Supriya, *Eur J Inorg Chem* 2021, 734–739.
(8) H. Y. Wang, S. R. Li, X. Wang, L. S. Long, X. J. Kong and L. S. Zheng, *Sci. China Chem*. 2021, **64**, 959–963.
(9) J. Lin, N. Li, S. Yang, M. Jia, J. Liu, X. M. Li, L. An, Q. Tian, L. Z. Dong and Y. Q. Lan, *J. Am. Chem. Soc*. 2020, **142**, 13982–13988.

==========